

Quantitative Phase Measurements Using a Quadrature Tomographic Microscope

Daniel J. Townsend^{a,d}, Kregg D. Quarles^b, Anthony L. Thomas^b, Willie S. Rockward^b,
Carol M. Warner^{a,c}, Judith A. Newmark^{a,c}, and Charles A. DiMarzio^{a,d}

^aCenter for Subsurface Sensing and Imaging Systems, Northeastern University,
Boston, MA 02115, USA

^bDepartment of Physics, Morehouse College, Atlanta, GA 30314, USA

^cDepartment of Biology, Northeastern University, Boston, MA 02115, USA

^dDepartment of Electrical and Computer Engineering, Northeastern University,
Boston, MA 02115, USA

ABSTRACT

The Quadrature Tomographic Microscope measures the amplitude and phase of an image. This information allows the user to see contrast features not available in other microscopes, and is critical to any three-dimensional reconstruction. We report on development and use of test objects to measure the accuracy and repeatability of phase measurements. A simple binary phase grating, a series of glass beads, and preimplantation mouse embryos were used in these experiments. The gratings were fabricated on high-quality fused-silica substrates whose transmission phase error was determined to be less than one-tenth wave error across their 25 mm diameter before fabrication. The phase step of the binary phase grating was measured using both the optical quadrature technique and the usual fringe-counting techniques applied to the raw data. Phase unwrapping techniques were validated by measuring the diameter of glass beads of a known size. Results are presented showing that the phase measurements agree with each other, with the known data, and with the spatial resolution in preimplantation mouse embryos. More complicated objects will be fabricated in the future to validate 3-D imaging techniques.

1. INTRODUCTION

It has been shown that the Quadrature Tomographic Microscope (QTM) successfully images the complex amplitude and phase of an optically transparent object.¹ The images taken with the QTM have been used to study the viability of mouse preimplantation embryos as a model system for eventual clinical application to human in vitro fertilization (IVF). The ability of the QTM to accurately report phase is reported in this paper.

Fused-silica targets were designed as test samples to test the accuracy of the QTM. These targets have known step sizes, and hence a known phase shift at a given wavelength. Therefore these targets can be used to measure the error of the phase images.

In addition, phase measurements of glass beads were made. Glass beads are a more realistic test target than the binary phase gratings, since most biological samples have curved features. We have begun using some established phase unwrapping algorithms to eliminate the 2π ambiguities inherent in phase images of curved objects taken with the QTM. To a good approximation unwrapped phase images yield the optical path length through a sample, the integrated product of index of refraction and depth or thickness. We will show phase unwrapping algorithms that provide new results that have applications in biological imaging.

Previously, the QTM was proposed as a method to image mouse embryos to assess viability.² The validation of QTM measurements using the test targets above is an important first step in the application of the QTM to biological imaging. Recent QTM images of various embryonic developmental stages have shown promise that the phase images yield more axial information than Differential Interference Contrast (DIC) microscopy. With this new axial information, non-destructive cell counting, which provides an indication of embryo health, should be possible.

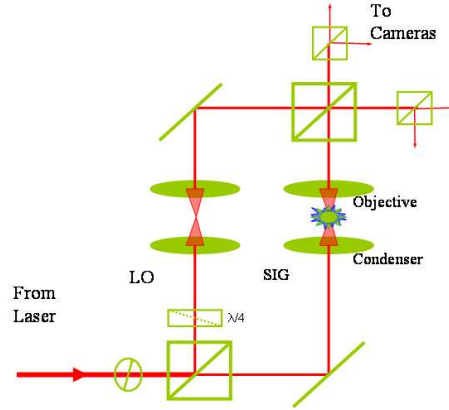


Figure 1. The Mach-Zehnder based design of the microscope. There are two paths for the light to follow. The local oscillator is circularly polarized and the signal path is polarized linearly at 45 degrees. This design allows for measurement of the in-phase and quadrature components of the field. The use of both interferometer outputs provides common-mode noise rejection.

2. OPTICAL QUATRATURE MEASUREMENTS

The principles of QTM have been reported previously,³ but we will briefly review the important concepts. For imaging, the quadrature tomographic microscope uses a technique similar to RF quadrature detection/mixing. The microscope employs a low-power HeNe laser for a light source ($\lambda = 633 \text{ nm}$). The microscope setup is similar to a Mach-Zehnder Interferometer (Figure 1). The laser beam is split into two paths, the local oscillator and the signal path. The local oscillator path includes a 45 degree linear polarizer and a quarter-wave plate to yield a circularly polarized beam, while the signal path is linearly polarized at 45 degrees. The two beams are then passed through a recombiner and two polarizing beam cubes.

The microscope was built upon a Nikon 200 platform.⁴ All images were taken with a 20X objective with a numerical aperture (NA) of 0.45. Images are captured by four synchronized Sony X-75 CCD cameras. Resolution for images is $0.33 \mu\text{m}$ per pixel, with images of 640×480 pixels. The total field of view for images is $160 \mu\text{m}$ by $120 \mu\text{m}$. A 15mW HeNe light source was used in the Mach-Zehnder design, with a single mode fiber splitting between the local oscillator and signal paths. The single mode fiber spatially filters the laser beam. This allows for easier alignment and serves as a better illumination source than a beam in free space.

The four images collected by the CCD cameras are given by the following equations:

$$\begin{cases} \text{Camera 0: } |E_0|^2 = |E_{sig}|^2 + |E_{ref}|^2 + 2\Re(E_{sig}E_{ref}^*) \\ \text{Camera 1: } |E_1|^2 = |E_{sig}|^2 + |E_{ref}|^2 + 2\Im(E_{sig}E_{ref}^*) \\ \text{Camera 2: } |E_2|^2 = |E_{sig}|^2 + |E_{ref}|^2 - 2\Re(E_{sig}E_{ref}^*) \\ \text{Camera 3: } |E_3|^2 = |E_{sig}|^2 + |E_{ref}|^2 - 2\Im(E_{sig}E_{ref}^*) \end{cases}. \quad (1)$$

The complex amplitude of the image is obtained by several steps. The first is recording the reference and signal mixed together. Then, by a sequence of blocking the reference and signal paths, we subtract out the signal and reference terms. This leaves only the cross terms of the combined electric field of the reference and signal. As shown in Equation (2), by dividing out the square root of the reference, the remaining term is the signal (complex amplitude) desired:

$$\hat{E} = \sum_{k=0,1,2,3} \frac{E_{mix} - E_{ref} - E_{sig}}{\sqrt{E_{ref}}}. \quad (2)$$

After extracting the complex amplitude of the image, using the technique above, the phase is found by:

$$\phi = \tan^{-1} \left(\frac{\Im(\hat{E})}{\Re(\hat{E})} \right). \quad (3)$$

3. IMAGES OF CALIBRATED GRATINGS AND GLASS BEADS

To make quantitative measurements with the quadrature tomographic microscope, both binary phase gratings and glass beads were used. The binary phase gratings were designed and manufactured at the Micro-Optics Research and Engineering Laboratory at Morehouse College, while the glass beads were purchased through a commercial source. Imaging was done on the QTM at the Optical Science Laboratory at Northeastern University.

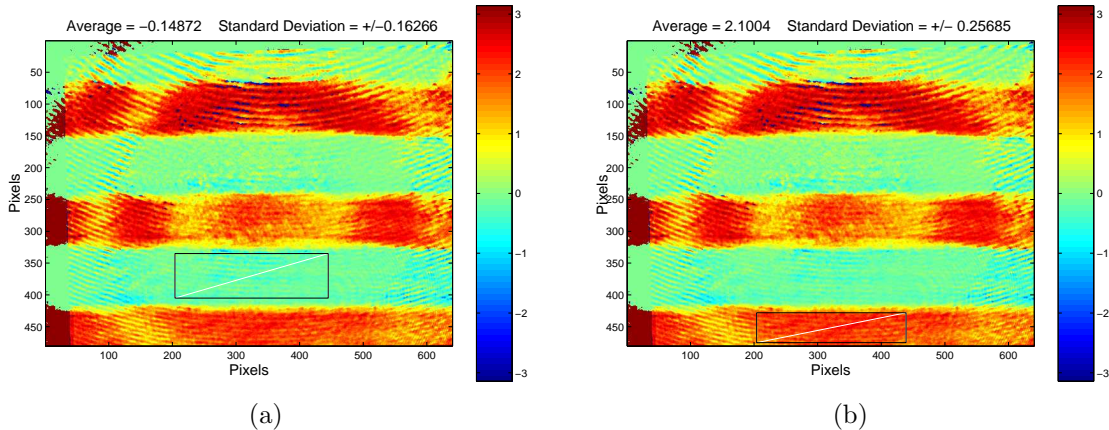


Figure 2. Phase images of a binary phase grating. The measured phase was done by spatially averaging at valley (a) and the peak (b) of the grating. The total phase change measured agrees closely with the actual phase.

3.1. Binary phase grating

The binary phase gratings were fabricated using techniques based on desktop-publishing and the Postscript page-layout language. The gratings were fabricated on high-quality fused-silica substrates whose transmission phase error was determined to be less than one-tenth wave error across their 25 mm diameter before fabrication. The surface structures were fabricated using standard photolithographic techniques. The pattern in photoresist was transferred onto the quartz substrate by chemical etching. Once the gratings were fabricated their surface structure [the grating period, the duty cycle (a ratio of the minimum feature to the period), the phase depth, and the overall profile] was measured with a Tencor AlphaStep 500 Surface Profileometer. The phase through the binary grating at 633 nm is 2.065 radians.

Figure 2 shows QTM phase images of the binary phase grating. In Figure 2a, the rectangular box represents the average phase change over the valley area of the grating. The average phase measured was -0.15 radians with a standard deviation of 0.16. In Figure 2b, the rectangular box represents the phase over the peak area of the grating. The average phase measured was 2.10 radians with a standard deviation of 0.26. Adding together the values for phase from the peaks and valleys of the binary grating gives a total phase shift of 2.25 radians. Comparing the actual phase change through the target (2.065 radians) with the measured phase change with the QTM (2.25 radians) we find that the error with our instrument is 0.18 radians or 10.55 deg. This error is acceptable for low resolution biological imaging of phase, such as imaging mouse embryos.

3.2. Glass Beads

In order to study more realistic test targets, we used glass beads to image phase. However, phase measurements of objects where Equation 4 holds will produce wrapped images.

$$\int n \cdot dl > \lambda \quad (4)$$

Wrapped phase images will yield 2π discontinuities in images (Figure 3a). Recently, we have used a two-dimensional phase unwrapping algorithm⁵ that eliminates the 2π discontinuities. In order to validate the phase unwrapping techniques, we used a glass bead with known diameter, 60 μm , and recorded phase measurements. All glass beads were immersed in water, with the index of refraction of the glass beads estimated at 1.45.

With an unwrapped phase image, the total phase change is indicative of a depth:

$$\phi = \frac{2\pi}{\lambda}z. \quad (5)$$

The image in Figure 3b shows the results of the unwrapping algorithm.

The unwrapped phase is relative in all QTM phase images. Unwrapped phase images will tend to differ in phase, due to varying path length in the interferometer and varying volume of liquid in which the objects are immersed. Therefore, a calculation for our sample thickness can be made using Equation (5). We see that the background phase is approximately -5 radians, while the center of the bead is approximately 63 radians. The total phase change through the glass bead is therefore 68 radians. Through the following relation:

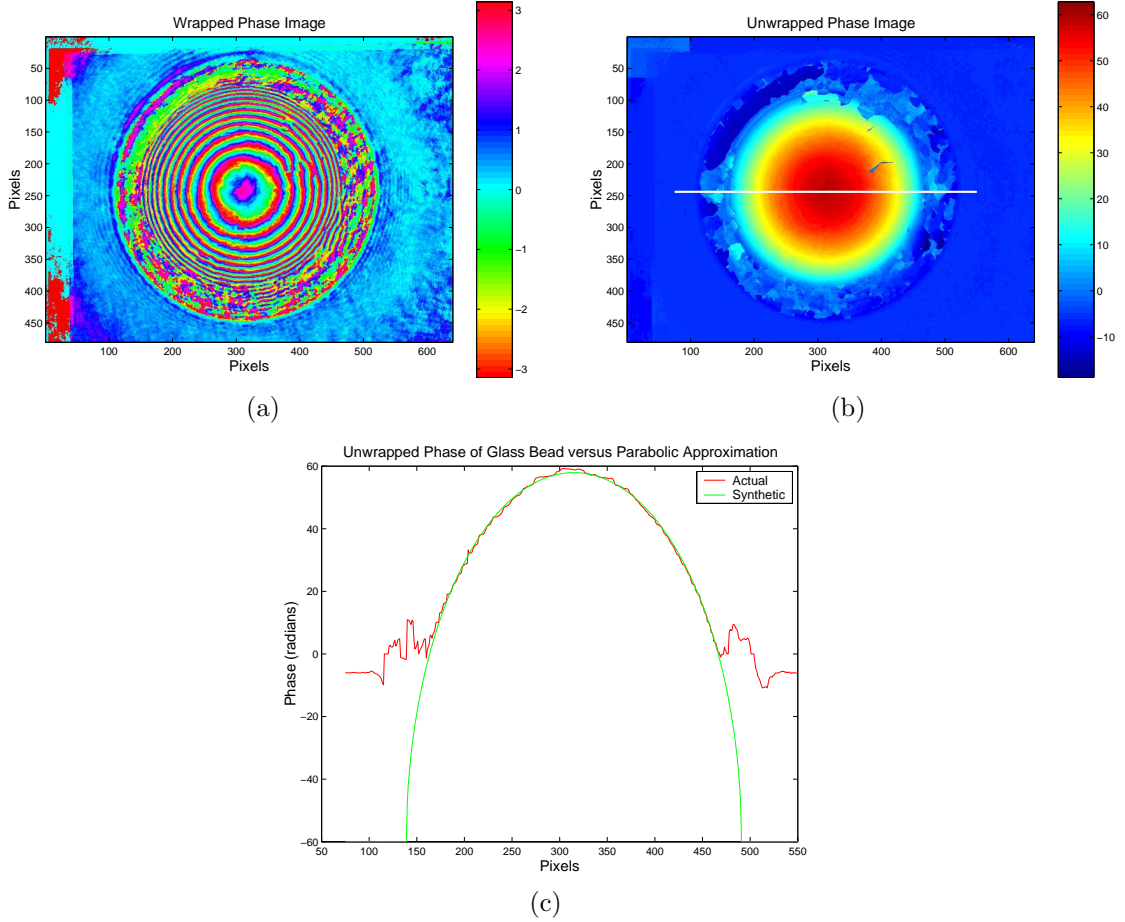


Figure 3. Panel (a) displays the wrapped image of a glass bead. The ringing in the image shows the 2π ambiguities that are inherent in phase images. Panel (b) displays the unwrapped image. Panel (c) shows the model prediction versus the actual data.

$$z_{glass} = \frac{\phi_{measured}\lambda}{2\pi(n_{glass} - n_{water})}, \quad (6)$$

we find the total thickness of this glass bead to be approximately $57 \mu\text{m}$. Knowing that the bead is spherical and approximately $60 \mu\text{m}$ in diameter, the total thickness of the bead should also be $60 \mu\text{m}$. Thus, the QTM measures the thickness of a glass bead with an error of $3 \mu\text{m}$. This is the error we can expect in the type of low resolution biological images that are created with the QTM.

Furthermore, mathematical modeling agrees with the depth associated with the unwrapped phase images (unpublished data). We have created a model to approximate the phase with an ellipsoid shape. The approximation is given by:

$$\phi = 2\sqrt{r^2 - x^2}, \quad (7)$$

where ϕ is the predicted phase, r is the given radius of the glass bead, and x is the distance

associated with the line in Figure 3b. From this approximation, we get an ellipsoid shape that agrees with the corresponding slice through the unwrapped phase image shown in Figure 3c.

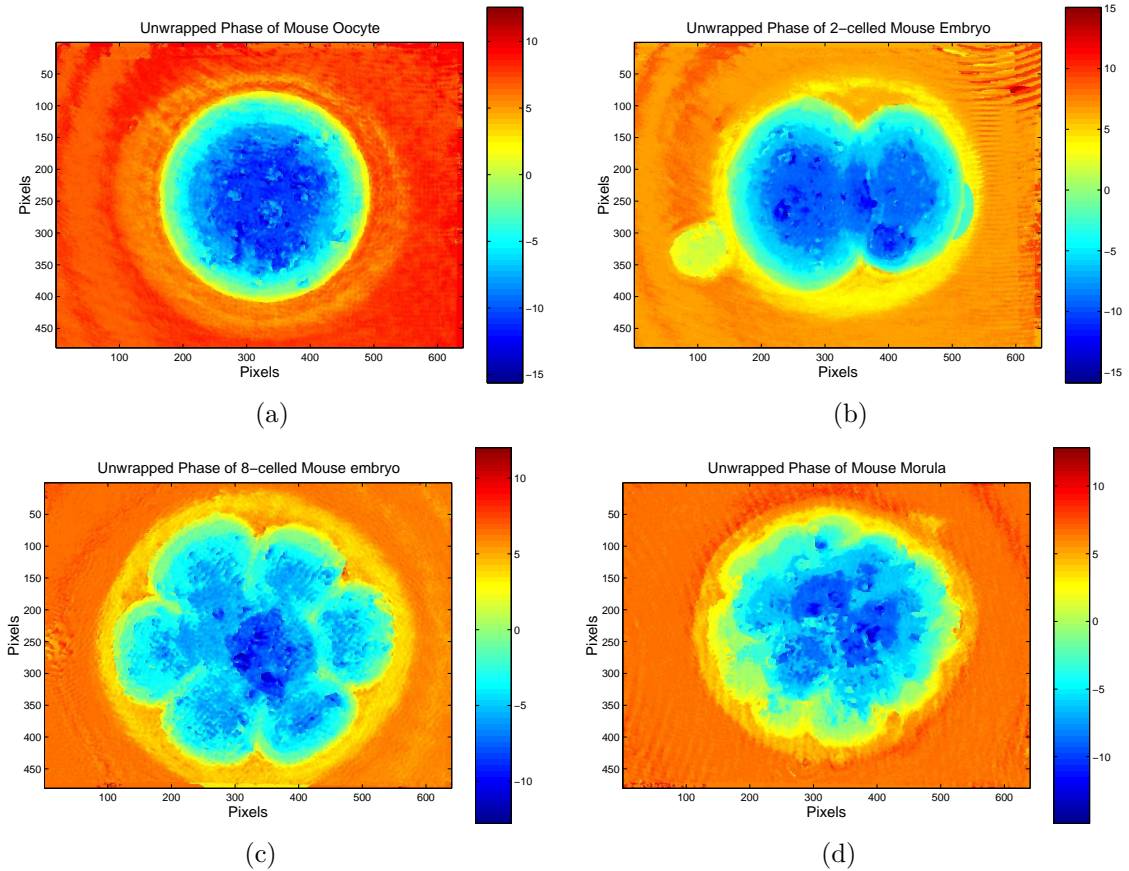


Figure 4. Unwrapped phase images taken with the Quadrature Tomographic Microscope of mouse embryos at different stages of development. Panel (a): oocyte. Panel (b): 2-cell embryo. Panel (c): 8-cell embryo. Panel (d): morula (a 16-cell embryo).

4. RECENT RESULTS IN BIOLOGICAL IMAGING

Since validation of the phase imaging, biological imaging with the QTM has continued. Prior reports have assessed the difference between young and old mouse oocytes (unfertilized eggs). Given the ability to make quantitative measurements on the optical path we have begun to concentrate on imaging multi-cell embryos. Recent work has shown that the embryo proliferation rate is correlated with embryo health.⁶ Embryos that develop at a fast rate are more likely to give rise to viable offspring. Phase measurements were recorded throughout the various stages of embryo development [oocyte, 2-cell, 8-cell, and morula (16-cell) stage embryos]. Phase measurements indicate that there is some axial distinction related to the number of cells, based upon the unwrapped phase images. This is expected because the Quadrature Tomographic Microscope reports the phase as the total change of index of refraction along an optical path length.

$$\phi = \int \Delta k n d l \quad (8)$$

In Figure 4, where two or more cells overlap there are more contributions to the phase. Using the outside of the cell as a reference, and looking at regions of greater phase change in the image, the Δk can be found. For instance, using the 8-cell embryo (Figure 4c), three different contributions are evident. First, the background lies at approximately 5 radians. Looking at the edges of the cell, where there is only one cell, the phase is -4 radians. In the middle of the cell, where there is suspected stacking of cells, the highest phase is reported at approximately -13 radians. Hence, there are even multiples of phase changes going from areas where there are no cells to one cell, and one cell to two cells.

QTM images should be useful to biologists because they provide insight into what is below the visible surface of the embryo. Currently, imaging of embryos is typically performed with the DIC technique. This technique provides excellent contrast on the surface, however, it gives incomplete information from the interior of the embryo.

5. FUTURE WORK

Further validation of phase measurements will be made through modeling. Initial results show that a finite difference time domain model agrees with unwrapped phase results (unpublished data). More complicated phase gratings with larger and nearly continuous phase variations are being fabricated. Similar measurements with spatial averaging will be compared with the expected results.

More biological tests will be made, with emphasis on cell counting. Speedup of image capture and processing will allow for statistical analysis, with emphasis on number of cells versus time. Furthermore, fluorescence images of stained nuclei of embryos will yield the correct number of cells to validate our QTM measurements. Our hypothesis that the Quadrature Tomographic Microscope can count cells in unstained embryos will be verified.

6. CONCLUSIONS

Through calibrated test targets we have demonstrated the ability to make accurate phase measurements down to an acceptable error of 0.14 radians for wrapped phase images and 3 μm (when determining depth) for unwrapped phase images. With accurate phase unwrapping algorithms, we can now move to biological images with more assurance that our cell counting ability has been validated.

7. ACKNOWLEDGMENTS

This work was supported in part by CenSSIS, the Center for Subsurface Sensing and Imaging Systems, under the Engineering Research Centers Program of the National Science Foundation (award number EEC-9986821) and in part by NIH grants HD39215 and HD40309 (to C.M.W.).

REFERENCES

1. D. Hogenboom, C. DiMarzio, T. Gaudette, A. Devaney, and S. Lindberg, "Three-dimensional images generated by quadrature interferometry," *Applied Optics* **23**, pp. 783–785, 1998.
2. Y. Glina, G. Tsihrintzis, C. Warner, D. Hogenboom, and C. DiMarzio, "On the use of the optical quadrature method in tomographic microscopy," in *Three Dimensional and Multidimensional Microscopy: Image Acquisition and Processing VI*, T. W. Jose-Angel Conchello, Carol J. Cogswell, ed., *Proceedings of SPIE* **3605**, pp. 101–106, 1999.

3. J. Stott, R. Bennett, C. Warner, and C. DiMarzio, "Three-dimensional imaging with a quadrature tomographic microscope," in *Three-dimensional and Multidimensional Microscopy: Image Acquisition and Processing VIII*, T. W. Jose-Angel Conchello, Carol J. Cogswell, ed., *Proceedings of SPIE* **4261**, 2001.
4. C. DiMarzio, J. Corporon, C. Warner, and J. Newmark, "Advances in development of a quadrature tomographic microscope," in *OSA Biomedical Topical Meetings*, pp. MG4-1 – MG4-3, 2002.
5. D. Ghiglia and M. Pritt, *Two-Dimensional Phase Unwrapping: Theory, Algorithms, and Software*, John Wiley and Sons, New York, 1998.
6. C. Warner and C. Brenner, "Genetic regulation of preimplantation embryo survival," *Current Topics in Developmental Biology* **51**, pp. 151–192, 2001.